Letter

Universal coherent atom-molecule oscillations in the dynamics of the unitary Bose gas near a narrow Feshbach resonance

Ke Wang [1,2] Zhendong Zhang,[3] Shu Nagata [1] Zhiqiang Wang [1,4,5,6] and K. Levin[1]

[1]*Department of Physics and James Franck Institute, University of Chicago, Chicago, Illinois 60637, USA*

[2]*Kadanoff Center for Theoretical Physics, University of Chicago, Chicago, Illinois 60637, USA*

[3]*E. L. Ginzton Laboratory and Department of Applied Physics, Stanford University, Stanford, California 94305, USA*

[4]*Hefei National Research Center for Physical Sciences at the Microscale and School of Physical Sciences, University of Science and Technology of China, Hefei, Anhui 230026, China*

[5]*Shanghai Research Center for Quantum Science and CAS Center for Excellence in Quantum Information and Quantum Physics, University of Science and Technology of China, Shanghai 201315, China*

[6]*Hefei National Laboratory, University of Science and Technology of China, Hefei 230088, China*

Quench experiments on a unitary Bose gas around a broad Feshbach resonance have led to the discovery of universal dynamics. This universality manifests in the measured atomic momentum distributions, where, asymptotically, a quasiequilibrated metastable state is found in which both the momentum distribution and the timescales are determined by the particle density. In this Letter we present counterpart studies for the case of a very narrow Feshbach resonance of ^{133}Cs atoms with a width of 8.3 mG. In dramatic contrast to the behavior reported earlier, a rapid quench of an atomic condensate to unitarity is observed to ultimately lead to coherent oscillations involving dynamically produced condensed and noncondensed molecules and atoms. The same characteristic frequency, determined by the Feshbach coupling, is observed in all types of particles. To understand these quench dynamics and how these different particle species are created, we develop a beyond Hartree-Fock-Bogoliubov dynamical framework including a type of cross-correlation between atoms and molecules. This leads to quantitative consistency with the measured frequency. Our results, which can be applied to the general class of bosonic superfluids associated with narrow Feshbach resonances, establish a alternate paradigm for universal dynamics dominated by quantum many-body interactions.

Introduction. Understanding the inherently unstable unitary Bose gas has remained a challenge [1–6]. Some progress, however, has been made, principally because rapid field sweeps across a Feshbach resonance to unitarity show, fortuitously, that the gas lives long enough to reveal features of quasisteady-state behavior before inevitable losses set in. This is seen through the momentum distribution $n(k)$ of noncondensed particles [7,8], which are associated with nonzero momentum. Importantly, these sweeps establish that the signal at high momentum k grows and eventually saturates as a function of time. These intriguing saturation phenomena have been referred to as a form of prethermalization [9,10]. Interestingly, for the systems studied thus far, the timescale for such quasisteady-state dynamics is claimed to be universal. As the scattering length $a_s \to \infty$, it is presumed that time-dependent phenomena should be determined by the remaining energy scale $E_F \propto (6\pi^2 n)^{2/3}$ [11–17], where n is the density of bosons.

Here we emphasize that this form of universality does not apply to the narrow resonance case. Even at unitarity, the relevant energy scale corresponds to the many-body Feshbach coupling $\alpha\sqrt{n}$, which should be contrasted with the Fermi energy E_F. This scale may be ignored in previous work [7,8] since there $\alpha\sqrt{n} \gg E_F$. However, the dynamics of the unitary gas in this narrow resonance regime, which has not received the same degree of attention, remains to be experimentally characterized and theoretically understood.

In this Letter, using both theory and experiment, we investigate the case of this narrow Feshbach resonance. In contrast to previous Bose gas studies which focused on the atoms, we have access to a sizable population of closed channel molecules which govern much of the physics at unitarity. Our work is motivated by an earlier observation of the effective temperature T_{eff} of out-of-condensate atoms and of closed channel molecules [18], which is plotted in Fig. 1. They are created during a quench to unitarity of an atomic Bose-Einstein condensate (BEC) of ^{133}Cs atoms associated with a narrow resonance (of width 8.3 mG). Although oscillations in T_{eff} were not reported previously, they are revealed here based on an error bar weighted fit to the temperature-dependent data.

It is our goal to experimentally investigate and theoretically understand the initial creation and subsequent oscillatory dynamics of these excited atomic and molecular states. To
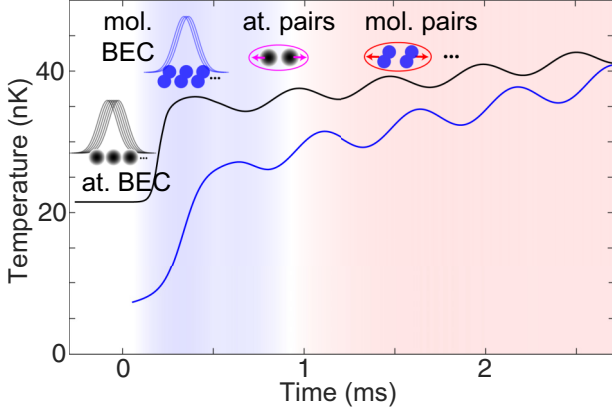
FIG. 1. Effective temperature of atoms (black solid line) and molecules (blue) based on an error bar weighted fit to data from Ref. [18] emphasizing the creation of out-of-condensate particles derived from an atomic BEC after a quench to unitarity (see the Supplement Material [19]). The small cartoons indicate the different species of particles generated at different stages of the dynamics, including atomic and molecular BECs and finite-momentum atomic and molecular pairs.

this end, we employ a time-of-flight (TOF) procedure. By analyzing a dataset from previous experiments [18,20], we are able to characterize multiple new observables. They include the atomic and molecular particle number distributions at different momenta and their associated kinetic energies [19].

Theoretically, to understand the oscillatory behavior observed in these quantities, we go beyond the Hartree-Fock-Bogoliubov [21,22] approach and establish a alternate dynamical framework that includes atom-molecule correlations. These correlations, which have no counterpart in the broad resonance case, turn out to be central to the dynamics of out-of-condensate particles. In the process we identify three distinct evolutionary stages in the quench dynamics; they are initiated by the generation of a molecular Bose-Einstein condensate (BEC) and subsequently followed by the creation of finite-momentum atoms and molecules which then undergo coherent oscillations [18,23,24]. Satisfactory quantitative agreement is obtained between theory and experiment both for the rather large oscillatory frequency which turns out to be around 2 kHz and for the net increase of kinetic energy (associated with the decay of the initial atomic condensate) which is transferred to newly excited atoms and molecules.

Dynamical framework. The effective Hamiltonian for a magnetic Feshbach resonance is associated with coupling between atomic and molecular channels (respectively called "open" and "closed"). It is given by

$$\hat{H} = \sum_\sigma \int d^3x \, \hat{\psi}_\sigma^\dagger(x) \left(-\frac{\hbar^2 \nabla^2}{2m_\sigma} + \nu_\sigma \right) \hat{\psi}_\sigma(x)$$

$$+ \int d^3x \sum_\sigma \frac{g_\sigma}{2} \hat{\psi}_\sigma^\dagger \hat{\psi}_\sigma^\dagger \hat{\psi}_\sigma \hat{\psi}_\sigma - (\alpha \hat{\psi}_1^\dagger \hat{\psi}_1^\dagger \hat{\psi}_2 + \text{H.c.}).$$

(1)

Here $\sigma = 1, 2$ represent the atoms and molecules, respectively, and $\nu_\sigma = \delta_{\sigma,2}\nu$, where ν is the detuning; g_σ is

proportional to the background *s*-wave interaction, and α corresponds to the important Feshbach coupling [25] strength between the two channels. Model parameters are related to the physical quantities by $g_\sigma = 4\pi\hbar^2 a_\sigma/(\Gamma_\sigma m_\sigma)$ and $\alpha = \Gamma_1^{-1}\sqrt{2\pi\hbar^2 a_1 \delta\mu \Delta B/m_1}$, and Γ_σ is $1 - 2a_\sigma\Lambda/\pi$. Here a_1 and a_2 are the background scattering lengths of atoms and molecules, $\delta\mu$ is the relative magnetic moment between open and closed channels, and ΔB is the resonance width. The detuning ν is related to the physical detuning $\nu_r = \delta\mu\delta B$ by $\nu = \nu_r + \Lambda m_1 \Gamma_1 \alpha^2/(\pi^2\hbar^2)$, where δB is the distance of the magnetic field from the resonance. Here Λ is a regularization cutoff, chosen here as $a_1\Lambda = \pi/10$, although the results are not sensitive to the specific numerical value. We use experimental values [18] for the parameters $a_1, a_2, \delta\mu$, and ΔB to determine g_1, g_2, and α and the initial atomic density n in simulations [19].

To theoretically study nonequilibrium dynamics, we focus on one- and two-point equal-time correlations as dynamical variables [26–28]. The one-point correlation $\xi_\sigma(t) = V^{-1/2}\langle\hat{\psi}_\sigma(k=0,t)\rangle$ represents the atomic or molecular condensate wave function, and $c_\sigma \equiv |\xi_\sigma(t)|^2$ represents the condensate density. Operators representing the excitations are then given by $\hat{\psi}_\sigma'(k) = \hat{\psi}_\sigma(k) - \delta_{k,0}\sqrt{V}\xi_\sigma(t)$.

It is convenient to introduce a four-vector field operator, $\hat{\Psi}(k) = [\hat{\psi}_1'(k), \hat{\psi}_1'^\dagger(-k), \hat{\psi}_2'(k), \hat{\psi}_2'^\dagger(-k)]$. The quantum fluctuations that involve the finite-momentum particles correspond to two-point correlation functions, $G_{\alpha\beta}(k) = \langle\hat{\Psi}_\alpha(-k)\hat{\Psi}_\beta(k)\rangle$, from which we deduce physical quantities. The variables $n_1(k) \equiv G_{21}(k)$ and $n_2(k) \equiv G_{43}(k)$ represent the particle number associated with finite-k atoms and molecules. The interspecies correlations $G_{13}(k)$ and $G_{23}(k)$, which are central to the dynamics, are important: $G_{13}(k)$ is associated with the molecular pairs, and $G_{23}(k)$ controls the particle flow which results in the creation of finite-k molecules.

The dynamical equations associated with these correlation functions are readily derived in terms of coupling constants g_1, g_2, and α, which are, in turn, defined in terms of physical scattering lengths and the resonance width associated with the Hamiltonian in Eq. (1). These equations are given by

$$i\partial_t \xi_1 = 2g_1 n_1 \xi_1 + (g_1\xi_1^2 + g_1 x_1 - 2\alpha\xi_2)\xi_1^* - 2\alpha f_{12},$$

$$i\partial_t \xi_2 = (\nu + 2g_2 n_2)\xi_2 + (g_2\xi_2^2 + g_2 x_2)\xi_2^* - \alpha(x_1 + \xi_1^2). \quad (2)$$

Here $n_\sigma = \sum_{k\neq0} n_\sigma(k)/V$ is the density of out-of-condensate atoms and molecules, which includes all finite-k population of atoms and molecules, and V is the volume. We define $x_1 = \sum_{k\neq0} G_{11}(k)/V$ and $x_2 = \sum_{k\neq0} G_{33}(k)/V$, which represent atom and molecule pairs, respectively, as discussed in the Supplemental Material [19]. Additionally $f_{12} = \sum_k G_{23}(k)/V$ characterizes the atom-molecule correlation function, which plays a centrally important role. The equations of motion for the two-point correlations can be compactly written as

$$i\partial_t G_{mn}(k) = \sum_\beta L_{m\beta}(k)G_{\beta n}(k) + L_{n\beta}(k)G_{m\beta}(k), \quad (3)$$

where $L(k)$ represents the coupling between finite-momentum atoms and molecules [19]. This dynamical scheme should be contrasted with the standard Hartree-Fock-Bogoliubov
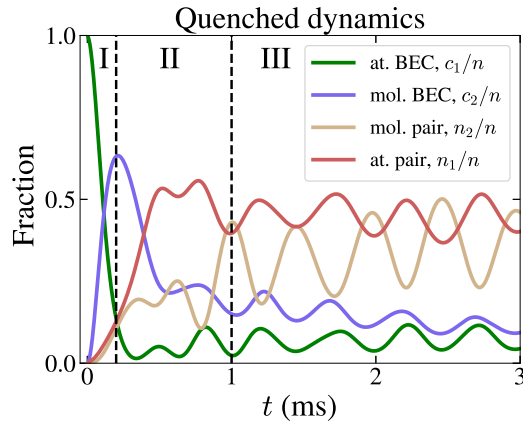
FIG. 2. Population transfers and growth in the present theory. When an atomic BEC is quenched to unitarity, a molecular BEC is the first to be created. After $t = 0.2$ ms, both atomic and molecular BECs decay, generating a large fraction of noncondensed atoms and molecules. After 1 ms, all particles exhibit oscillations with identical frequency. Only the noncondensed molecules are out of phase because they control the flow of particles.

approach [21,22], which omits these new atom-molecule correlations such as f_{12}.

Three evolutionary stages. Using these dynamical equations, we identify different stages of particle creation throughout the quench dynamics. The quench of an atomic BEC to unitarity is implemented by an abrupt change in the detuning $\nu_r \sim 0$ assuming that, initially, at $t = 0$, all particles reside in an atomic BEC. As indicated in Fig. 2 in stage I, Feshbach couplings convert the initial atomic condensate into a coherent molecular BEC along with a small number of atomic and molecular pairs with momentum $\pm k$ [29]. In stage II, shortly after its formation, the molecular BEC begins to partially decay, and more atomic pairs appear. The latter in turn combine with an atom from the condensate to form an atom-molecule complex. The combination of an atom-molecule complex and an atom from the condensate is further converted into a pair of molecules. In stage III, with these finite-momentum atomic and molecular populations now fully formed, the system enters a stage of steady-state coherent oscillations.

What is particularly interesting about these oscillations is that, at unitarity, there is an in-phase relationship between all quantities except for the noncondensed molecules. This phenomenon derives from a competition involving the three particle currents driven by the Feshbach coupling [19]. These currents represent the flow of particles between atoms and molecules and condensates. Our central finding is that at resonance, once noncondensed molecules are created, they tend to control (through the equations of motion) the general dynamics of the particles. As a consequence, the out-of-condensate molecules are, interestingly, out of phase with the other three species [19].

Most of the general observations we outline below (unless indicated otherwise) pertain to both theory and experiment [30], and a comparison is presented in Fig. 3. As is suggested by Fig. 1, we see here that the newly generated out-of-condensate particles which carry kinetic energy are associated with oscillatory dynamics. As the atomic condensate
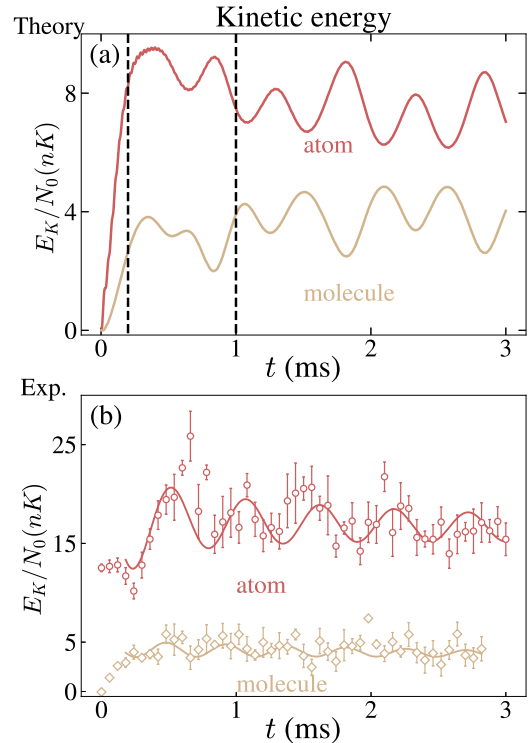

FIG. 3. Kinetic energy variation E_K/N_0 of atoms and molecules, which is associated with the population transfers and growth in Fig. 2. Here $E_K^\sigma/N_0 \equiv \int d^3k/(2\pi)^3 n_\sigma(k)(k_x^2 + k_y^2)/(2m_\sigma n)$. (a) Theory and (b) experiment. In experiment (but not theory) there is a loss of particles which is associated with a gain in kinetic energy, but the two effects tend to at least partially compensate in the plot. Experiment and theory show similar oscillatory behavior, and both show a net increase of kinetic energy which is of the order of 5 nK times N_0, where N_0 represents the total number of particles at the start of the sweep. We focus here on temperature variations which are comparable, noting that there are differences in the absolute values, presumably because the experiments are at finite T while the theory is at $T = 0$. Thus, while (a) and (b) show some quantitative differences, it is reasonable that the occupation of more and higher-momentum states seen in experiment may reflect thermal effects.

decays, a portion of its interaction energy is transferred to noncondensed particles. This leads to an increase of the kinetic energy in both atoms and molecules immediately after the quench at $t < 0.5$ ms. We can quantify this increase, E_K^σ/N_0, which is of the order of 10 nK for the atoms and 5 nK for the molecules, as found in both theory and experiment.

After the initial growth period, the oscillations notably persist for a period of around 2 ms, without any sign of thermalization. This oscillatory frequency is around 2 kHz, which, importantly, coincides with that of the population oscillations (see Fig. 2) [18]. Indeed, this single oscillation pattern observed in all collective observables reflects the fact that the same underlying microscopic dynamical processes are present.

Momentum-resolved distributions and asymptotic coherent oscillations. Of interest next is to clarify the microscopic mechanism responsible for the generation of finite-momentum particles after the initial formation of the molecular BEC. This is associated with the Feshbach resonant
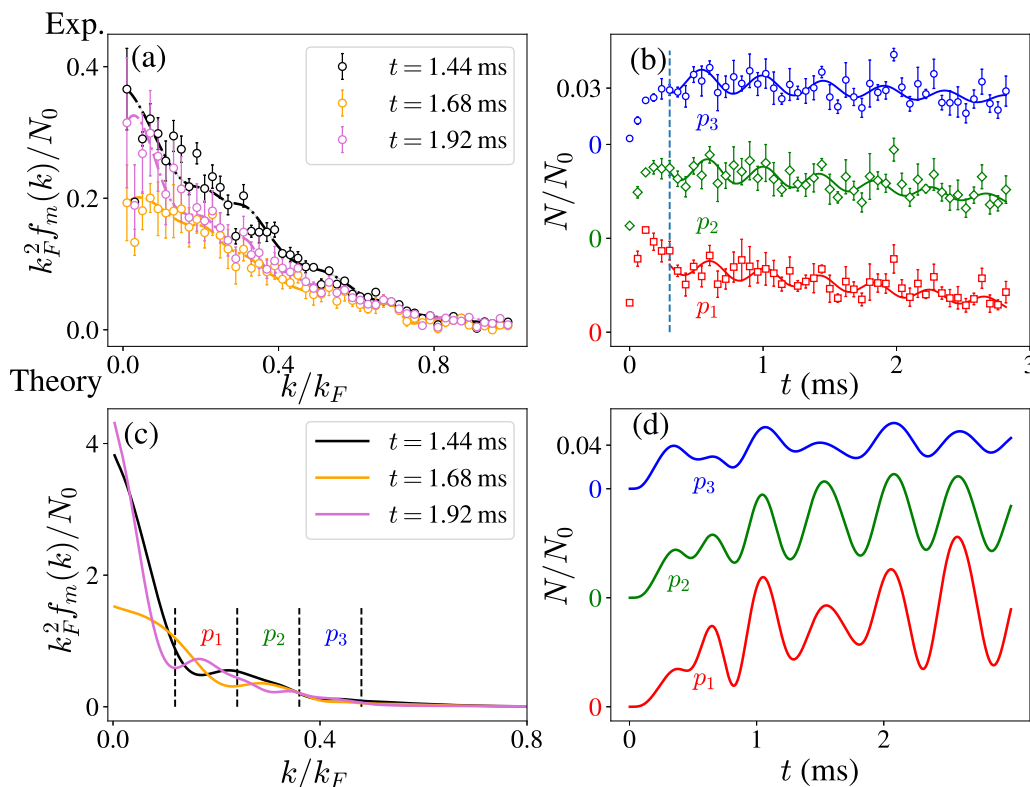
FIG. 4. Theory-experiment comparison of the dynamics of finite-momentum molecules, where (a) represents the experimentally measured momentum distribution f_m at three different times showing nonmonotonicity; the ordering of the curves from top to bottom corresponds to early, late, and intermediate time. Here f_m is the angular average momentum distribution of molecules such that $\int d^2k f_m = N_m$. (b) plots their number vs time t when summed over a momentum shell. The summation region is indicated by $p_1/p_2/p_3$. Here $p_i = \int_{k_i \leqslant k < k_{i+1}} d^2k f_m(k)$, where $k_i = 0.12k_F \times i$. (c) and (d) are the counterpart theory plots. We observe coherent oscillations in three different shells, all with the same frequency of 2kHz, in both theory and experiment. Comparing (a) and (c) suggests that the occupation of more and higher-momentum states seen in experiment may reflect thermal effects: The experiments are performed at finite T, whereas theory is at $T = 0$.

interaction and is contained in the properties of the matrix $L(k)$ in Eq. (3). The eigenvalues of L determine the speed of growth of these out-of-condensate particles, while the eigenvectors determine the fraction of atoms and molecules involved in the generation process [31]. We consider the eigenvalues of $L(k)$,

$$\lambda_\pm \simeq \sqrt{F_1(k) \pm \sqrt{F_1^2(k) - 4F_2(k)}}. \quad (4)$$

Here F_1 and F_2 are given by $F_1(k) = \epsilon_1^2(k) + \epsilon_2^2(k) + 8\alpha^2|\xi_1|^2 - 4\alpha^2|\xi_2|^2$ and $F_2(k) = [\epsilon_1(k)\epsilon_2(k) - 4\alpha^2|\xi_1|^2]^2 - 4\alpha^2|\xi_2|^2\epsilon_2^2(k)$. Here we have introduced the dispersion $\epsilon_\sigma(k) = k^2/2m_\sigma + \nu_r\delta_{2,\sigma}$. One may observe that two circumstances exist which lead to an imaginary λ and a consequent instability of condensates: either $F_1(k) < 0$, which is associated with the processes in stage I, or $F_2(k) < 0$, which is mainly associated with those processes in stage II. These unstable outcomes are *unavoidable* when particles mostly reside in condensates. Indeed, once a molecular condensate is present ($\xi_2 \neq 0$), one can always find a value of k such that $\epsilon_1\epsilon_2 - 4\alpha^2|\xi_1|^2 \simeq 0$, leading to an imaginary value for λ_-. Additionally, for $|\xi_2| \gg |\xi_1|$, the instability occurs at $\epsilon_1^2(k) + \epsilon_2^2(k) < 4\alpha^2|\xi_2|^2$. In this way, finite-momentum particles are exponentially generated.

All of this can be contrasted with the larger k regime where the eigenvalues are real and there is, consequently, no significant occupation of those higher-momentum states, having k of the order of, say, k_F. Here the kinetic oscillations, rather than the exponential growth, dominate. Indeed, the momentum distributions we observe are consistent with the above analysis, where particles are seen to be concentrated in states with low momentum up to $\approx k_F/2$, where $k_F \equiv (6\pi^2 n)^{1/3}$. We stress that, in contrast to the saturation effects seen in the broad Feshbach resonance [7,8], the momentum distributions in the narrow resonance case oscillate during the later time dynamics, as seen in Figs. 4(a) and 4(c).

To confirm that a single oscillation frequency is present in the experiments, as suggested by theory, we determine the molecular population in a shell including different groupings of momenta p_i, as in Fig. 4. Three such subsets were considered, and the behavior in all is found to be rather similar, with all showing the characteristic frequency of 2 kHz. This shared common frequency between finite-momentum atoms and molecules and their condensates should be understood to derive from Feshbach coupling [19]. We note parenthetically that the amplitude of the oscillations is slightly greater in theory than experiment, which we attribute to finite-temperature effects in our experiment that suppress the coherence of atoms and molecules.

A final challenge we must address is to understand the microscopic origin of the ubiquitous 2 kHz oscillation frequency. Notably, a frequency of this order is a large energy scale compared to other energy scales in the problem, including the self-interaction energy terms deriving from g_1 and g_2, which are of the order of $E_g/h \equiv g_{1/2}n \simeq 0.25$ kHz. Determining where this large frequency originates requires evaluating the separation of the energy levels between atomic and molecular condensates. We are able to identify the main contribution to this energy gap as coming from the atom-molecule interspecies correlation f_{12}. This provides an additional self-energy correction to the atomic condensate $\mu_1 = -2\alpha \mathrm{Re}\, f_{12}/\xi_1$, arising from the Feshbach coupling $\sim \alpha \hat{\psi}_1^\dagger(x)\hat{\psi}_1^\dagger(x)\hat{\psi}_2(x)$ [see Eq. (3)]. Similarly, one finds the self-energy correction to the molecular condensate, $\mu_2 = -\alpha \mathrm{Re}\, x_1/\xi_2$. Together they determine the splitting of the atomic and molecular condensate levels: $\Delta\mu = 2\mu_1 - \mu_2$. It is notable that without this correction to μ_1, the characteristic oscillation frequency would be around 0.9 kHz [20]. But with these corrections, we find that $\Delta\mu$ is, indeed, around 2 kHz, bringing theory and experiment into reasonable agreement [19].

Conclusion. We emphasized throughout that the coherent oscillations we observe for the narrow resonance case are universal because they are determined by only a *single* energy scale $\alpha\sqrt{n}$. This leads to a different paradigm for the universal dynamics of the unitary Bose gas. This is associated with a many-body (Feshbach) coupling and should be contrasted with the universality previously discussed in the literature [7,8] and associated with the Fermi energy. As in the early literature, arriving at this universality required us to focus on characterizing the dynamical behavior of noncondensed particles which appear when an atomic condensate is swept to unitarity. Here in addition to atoms there are out-of-condensate molecules, and once they have formed, all populations reach a steady oscillatory state; all finite-momentum particles are seen to have the same intrinsic oscillation frequency, which is the same as that of the condensate [20].

In this context, we presented a reasonably successful comparison between theory and experiment. Because of these quantitative correspondences we were able to glean support for a rather different dynamical theory. It should be contrasted with the more conventional Hartree-Fock-Bogoliubov approach [21,22]. Importantly, this dynamical machinery and its rich phenomenology should be relevant to the general class of bosonic superfluids associated with narrow Feshbach resonances.

[1] S. B. Papp, J. M. Pino, R. J. Wild, S. Ronen, C. E. Wieman, D. S. Jin, and E. A. Cornell, Bragg spectroscopy of a strongly interacting ^{85}Rb Bose-Einstein condensate, Phys. Rev. Lett. **101**, 135301 (2008).

[2] N. Navon, S. Piatecki, K. Günter, B. Rem, T. C. Nguyen, F. Chevy, W. Krauth, and C. Salomon, Dynamics and thermodynamics of the low-temperature strongly interacting Bose gas, Phys. Rev. Lett. **107**, 135301 (2011).

[3] S. E. Pollack, D. Dries, M. Junker, Y. P. Chen, T. A. Corcovilos, and R. G. Hulet, Extreme tunability of interactions in a ^{7}Li Bose-Einstein condensate, Phys. Rev. Lett. **102**, 090402 (2009).

[4] S. Piatecki and W. Krauth, Efimov-driven phase transitions of the unitary Bose gas, Nat. Commun. **5**, 3503 (2014).

[5] R. J. Wild, P. Makotyn, J. M. Pino, E. A. Cornell, and D. S. Jin, Measurements of Tan's contact in an atomic Bose-Einstein condensate, Phys. Rev. Lett. **108**, 145305 (2012).

[6] E. Braaten, D. Kang, and L. Platter, Universal relations for identical bosons from three-body physics, Phys. Rev. Lett. **106**, 153005 (2011).

[7] P. Makotyn, C. E. Klauss, D. L. Goldberger, E. A. Cornell, and D. S. Jin, Universal dynamics of a degenerate unitary Bose gas, Nat. Phys. **10**, 116 (2014).

[8] C. Eigen, J. A. P. Glidden, R. Lopes, E. A. Cornell, R. P. Smith, and Z. Hadzibabic, Universal prethermal dynamics of Bose gases quenched to unitarity, Nature (London) **563**, 221 (2018).

[9] X. Yin and L. Radzihovsky, Publisher's Note: Postquench dynamics and prethermalization in a resonant Bose gas [Phys. Rev. A **93**, 033653 (2016)], Phys. Rev. A **94**, 039901(E) (2016).

[10] A. Rançon and K. Levin, Equilibrating dynamics in quenched Bose gases: Characterizing multiple time regimes, Phys. Rev. A **90**, 021602(R) (2014).

[11] S. Cowell, H. Heiselberg, I. E. Mazets, J. Morales, V. R. Pandharipande, and C. J. Pethick, Cold Bose gases with large scattering lengths, Phys. Rev. Lett. **88**, 210403 (2002).

[12] J. L. Song and F. Zhou, Ground state properties of cold bosonic atoms at large scattering lengths, Phys. Rev. Lett. **103**, 025302 (2009).

[13] Y.-L. Lee and Y.-W. Lee, Universality and stability for a dilute Bose gas with a Feshbach resonance, Phys. Rev. A **81**, 063613 (2010).

[14] J. M. Diederix, T. C. F. van Heijst, and H. T. C. Stoof, Ground state of a resonantly interacting Bose gas, Phys. Rev. A **84**, 033618 (2011).

[15] W. Li and T.-L. Ho, Bose gases near unitarity, Phys. Rev. Lett. **108**, 195301 (2012).

[16] S.-J. Jiang, W.-M. Liu, G. W. Semenoff, and F. Zhou, Universal Bose gases near resonance: A rigorous solution, Phys. Rev. A **89**, 033614 (2014).

[17] C. Gao, M. Sun, P. Zhang, and H. Zhai, Universal dynamics of a degenerate Bose gas quenched to unitarity, Phys. Rev. Lett. **124**, 040403 (2020).

[18] Z. Zhang, S. Nagata, K.-X. Yao, and C. Chin, Many-body chemical reactions in a quantum degenerate gas, Nat. Phys. **19**, 1466 (2023).

[19] See Supplemental Material at http://link.aps.org/supplemental/10.1103/PhysRevResearch.7.L012025 for the clarification of experimental-based parameters, the analysis of data, and the derivation of the dynamical equations.

[20] Z. Wang, K. Wang, Z. Zhang, S. Nagata, C. Chin, and K. Levin, Stability and dynamics of atom-molecule superfluids near a narrow Feshbach resonance, Phys. Rev. A **110**, 013306 (2024).

[21] S. J. J. M. F. Kokkelmans and M. J. Holland, Ramsey fringes in a Bose-Einstein condensate between atoms and molecules, Phys. Rev. Lett. **89**, 180401 (2002).

[22] V. D. Snyder, S. J. J. M. F. Kokkelmans, and L. D. Carr, Hartree-Fock-Bogoliubov model and simulation of attractive and repulsive Bose-Einstein condensates, Phys. Rev. A **85**, 033616 (2012).

[23] Y. Tian, Y. Zhao, Y. Wu, J. Ye, S. Mei, Z. Chi, T. Tian, C. Wang, Z.-Y. Shi, Y. Chen, J. Hu, H. Zhai, and W. Chen, Dissipation driven coherent dynamics observed in Bose-Einstein condensates, arXiv:2408.03815.

[24] V. G. Sadhasivam, F. Suzuki, B. Yan, and N. A. Sinitsyn, Parametric tuning of quantum phase transitions in ultracold reactions, Nat. Commun. **15**, 10246 (2024).

[25] R. A. Duine and H. T. C. Stoof, Atom–molecule coherence in Bose gases, Phys. Rep. **396**, 115 (2004).

[26] V. E. Colussi, H. Kurkjian, M. Van Regemortel, S. Musolino, J. van de Kraats, M. Wouters, and S. J. J. M. F. Kokkelmans, Cumulant theory of the unitary Bose gas: Prethermal and Efimovian dynamics, Phys. Rev. A **102**, 063314 (2020).

[27] M. Van Regemortel, H. Kurkjian, M. Wouters, and I. Carusotto, Prethermalization to thermalization crossover in a dilute Bose gas following an interaction ramp, Phys. Rev. A **98**, 053612 (2018).

[28] J. van de Kraats, D. J. M. Ahmed-Braun, V. E. Colussi, and S. J. J. M. F. Kokkelmans, Resonance triplet dynamics in the quenched unitary Bose gas, Phys. Rev. Res. **6**, L012056 (2024).

[29] The growth of this molecular BEC is associated with instanton dynamics: $\xi_2(t)/\sqrt{n} = i \tanh(t/t_\alpha)$, where $t_\alpha = \hbar/\alpha\sqrt{2n}$ [19].

[30] Because the experimentally observed particle loss is not significant within the 3 ms time frame [18], it makes sense to consider these comparisons.

[31] K. Wang, H. Fu, and K. Levin, Simulating cosmological evolution by quantum quench of an atomic Bose-Einstein condensate, Phys. Rev. A **109**, 013316 (2024).